Analytical model for three-dimensional Mercedes-Benz water molecules

T. Urbic

Phys. Rev. E **85**, 061503 — Published 25 June 2012

DOI: 10.1103/PhysRevE.85.061503

Analytical model for 3D Mercedes–Benz water molecules.

T. Urbic[1]

Faculty of Chemistry and Chemical Technology, University of Ljubljana, Askerceva 5, 1000 Lubljana, Slovenia

We developed a statistical model which describes the thermal and volumetric properties of water-like molecules. A molecule is presented as a three-dimensional sphere with four hydrogen-bonding arms. Each water molecule interacts with its neighboring waters through a van der Waals interaction and an orientation-dependent hydrogen-bonding interaction. This model, which is largely analytical, is a variant of a model developed before for a two-dimensional Mercedes-Benz model of water. We explored properties such as molar volume, density, heat capacity, thermal expansion coefficient and isothermal compressibility as a function of temperature and pressure. We found that the volumetric and thermal properties follow the same trends with temperature as in real water and are in good general agreement with Monte Carlo simulations, including the density anomaly, the minimum in the isothermal compressibility, and the decreased number of hydrogen bonds upon increasing the temperature.

I. INTRODUCTION

The structure and thermodynamics of water and aqueous solutions are of great importance for chemistry and biology. There is a long and rich history of modeling pure water, including Röntgen's two-density model from 1897[1], Pople's 1951 model of the bending of hydrogen bonds in a tetrahedral lattice[2], lattice and cluster models[3–13], treatments of water's unusual density behavior using double-well spherically symmetric potentials[14–17], treatments that begin with water's pair-correlation function or experimentally measured moments of distribution functions in place of a molecular potential[18–20]. In addition, there have been many computer simulations[21–23] including those based on multi-point classical force-field models such as SPC and TIP[24–28], or polarizable versions of them[29–32], as well as quantum mechanical treatments[33–35].

Despite significant work and progress in this area, the properties of water are still not well understood. Water is difficult to model because it forms hydrogen bonds, which can be described by orientation-dependent interactions. These interactions are coupled to each other rigidly and sterically (i.e., when a water molecule rotates, moving one hydrogen bonding arm, it rigidly moves all the other hydrogen bonding arms). This rigid internal orientational coupling of interactions leads to complex angular effects that are multi-body and nonlocal (a water molecule connects with other waters through networks, causing orientational correlations out to third and more distant neighbors), and such effects have been notoriously hard to treat. Water is often studied by computer simulations, but they are time expensive. It is difficult to explore waters entropies or heat capacities or effects of pressure, or water's pressure-temperature phase diagram using quantum-mechanical or atomically detailed computer simulations[36–38] because of the large amount of computational sampling required.

The aim of this work is to extend a statistical mechanical model we developed for a two dimensional (2D) Mercedes Benz model[39] to three dimensions (3D). A previous version of the model dates back to the early 1970s[40–43]. Recently, 3D Ben-Naim model was reinvented by Bizjak et al.[44,45] and Dias et al.[46,47] and studied using computer simulations[44–47] and integral equation theory[45]. According to 3D MB model, each water molecule is a Lennard–Jones sphere with four arms, oriented tetrahedrally to mimic formation of hydrogen bonds. Urbic and Dill's (UD) model is directly descendant from a treatment of Truskett and Dill (TD), who developed a nearly analytical version of the 2D MB model[48–50].

There exist also models which are extension of van der Waals equation with two microscopic states: hydrogen-bonded states (low density water) and van der Waals states (high density water) like model by Poole et al[51]. There is another group of lattice models[3,52,53] where water is presented as a lattice fluid in which bond formation depends strongly on molecular orientations and local density. These models are able to qualitatively reproduce the known thermodynamic behavior of water including the behavior of supercooled water and describe how the predictions of lattice-gas models are relevant to understanding liquid and amorphous solid water, but it is more difficult to use it for description of solvation effects. This model of MB water can be used to describe effect of solvation like it was recently done for two dimensional MB model[54].

The construction of this article is as follow: after the above-given Introduction, we show the extension of UD theory of water to 3D in Section 2. Theoretical and simulation results are reported, compared and discussed in Section 3. The last section highlights the main conclusions of this work.

II. THEORY

We consider a system of 3D MB model water molecules, modeled as 3-dimensional spheres. In the theory, we suppose that the structure of the liquid state of 3D model water is a perturbation from an underlying hexagonal (ice) lattice. Each molecule is located nearest to one particular grid point, and no two waters are assigned to the same point. For the purpose of keeping track of the state of interaction of all hydrogen bonding arms of each water molecule, we use as a bookkeeping tool an underlying ice lattice; see Figure 1. We focus on a single water molecule on the grid and the interaction of that water with its neighbor. Each molecule can be in one of three possible orientational states relative to its clockwise-like positioned neighbor on the lattice: (i) a water can be hydrogen-bonded, (ii) it can be in van der Waals contact, or (iii) it can have no interaction at all. These states are graphically presented in Figure 2. First we compute the isothermal-isobaric statistical weights, Δ_i, of the states as a functions of temperature, pressure, and interaction energies[39].

A. The hydrogen-bonded state

Here are the details how we represent the hydrogen bonded state and its Boltzmann factor. If the test water molecule points one of its four hydrogen bonding arms at an angle θ to within $\pi/3$ of the center of its neighbor water, it forms a hydrogen bond (see Figure 2). This is equivalent to about one fourth of full solid angle. The interaction energy of the test water with its neighbor is then

$$u_{HB}(\theta) = -\epsilon_{HB} - \epsilon_{LJ} + k_s(1+\cos\theta)^2, 0 < \theta < \pi/3 \tag{1}$$

ϵ_{HB} is an hydrogen bond energy constant representing the maximal strength of a hydrogen bond, ϵ_{LJ} is the Van der Waals contact energy between neighboring waters, and k_s is the angular spring constant that describes the weakening of the hydrogen bond with angle. We treat this type of hydrogen bond as weak bond[39] as it does not cooperate with neighboring hydrogen bonds. To compute the isothermal-isobaric partition function, Δ_{HB}, of this hydrogen bonded state, we integrate this Boltzmann factor over all the allowed Euler angles ϕ, θ and ψ and over all the allowed separations x, y and z of the test molecule relative to its clockwise neighbor,

$$\Delta_{HB} = c(T)\int\int\int\int\int dxdydzd\phi d\psi \int_0^{\pi/3} \sin\theta d\theta \exp\left(-(u_{HB} + pv_{HB}/2)/k_BT\right), \tag{2}$$

where $c(T)$ is the 3D version of the kinetic energy contribution to the partition function, k_B is Boltzmann's constant, T is temperature, p is the pressure, and v_{HB} is volume per molecule. The multiple integral $\int\int\int dxdydz$ represents the volume over which the second molecule has translational freedom to form a hydrogen bond with the first water and is equal to v_{ef}^{HB}. The double integral $\int\int d\phi d\psi$ sums the orientations over which the test molecule has orientational freedom and is equal to $4\pi^2$.

The volume v_{HB} of the hydrogen-bonded state is derived similarly as for the 2D model[39]. For the perfect hexagon crystal, representing low-pressure ice, the volume of the solid is

$$v_s = \frac{8\sqrt{3}r_{HB}^3}{9}, \tag{3}$$

We estimate volume v_{HB} as perturbation from this state as

$$x_v v_{HB} = v_s, \tag{4}$$

where $x_v = 1.12$ is chosen empirically because density of liquid state at room temperature is about 12 % more dense then ice.

Using these definitions and performing the integration in Equation (2) gives

$$\Delta_{HB} = 4\pi^2 c(T) v_{ef}^{HB} \exp\left(\frac{\epsilon_{HB} + \epsilon_{LJ} - p v_{HB}/2}{k_B T}\right) \sqrt{\frac{k_B T \pi}{4 k_s}} \mathrm{erf}\left(\sqrt{\frac{k_s}{4 k_B T}}\right). \tag{5}$$

B. The van der Waals state

In the vdW state, the test water molecule forms a contact with its clockwise-like positioned water, but no hydrogen bond. Energy of this state is

$$u_{LJ}(\theta) = -\epsilon_{LJ}, 0 < \theta < \pi/3 \tag{6}$$

The isothermal-isobaric partition function, Δ_{LJ}, of this state is given by integrating over angles and positions of the test particle relative to its clockwise neighbor,

$$\Delta_{LJ} = c(T) \int\int\int\int\int dx dy dz d\phi d\psi \int_0^{\pi/3} \sin\theta d\theta \exp\left(-(u_{LJ} + p v_{LJ}/2)/k_B T\right). \tag{7}$$

The volume v_{LJ} of this state is approximated as a volume of cubic close-packed crystal where the closest molecules at distance $\sigma_{LJ} 2^{1/6}$

$$v_{LJ} = \sigma_{LJ}^3. \tag{8}$$

The integral $\int\int\int\int\int dx dy dz$ represents the translation volume when second molecule forms van der Waals contact with first and is equal to effective volume v_{ef}^{LJ}. Integrating gives

$$\Delta_{LJ} = 2\pi^2 c(T) v_{ef}^{LJ} \exp\left(\frac{\epsilon_{LJ} - p v_{LJ}/2}{k_B T}\right) \tag{9}$$

C. The non-bonded state

In the last possible state, the test water molecule does not interact with its neighbors so the energy is

$$u_o(\theta) = 0. \tag{10}$$

The isothermal-isobaric partition function for the non-interacting state is obtained by integrating over translational degrees of freedom,

$$\Delta_o = c(T) \int\int\int\int\int dx dy dz d\phi d\psi \int_0^{\pi/3} \sin\theta d\theta \exp\left(-p v_o/2 k_B T\right), \tag{11}$$

where v_o is the volume available to the test molecule in this state. We compute v_o using the van der Waals gas approximation,

$$v_o = \frac{k_B T}{p} + v_{LJ}. \tag{12}$$

Integrating over all coordinates of this state gives

$$\Delta_o = 2\pi^2 c(T) \frac{k_B T}{p} \exp\left(\frac{-p v_o}{2 k_B T}\right) \tag{13}$$

D. Thermodynamic properties

Equations (5), (9) and (13) give the isobaric-isothermal ensemble Boltzmann weights of the three possible states of each water molecule. We assume the mean-field attractive energy,[55], $-Na/v$, among hexagons, where a is the van der Waals dispersion parameter (0.02)[39,48,49] and v is the average molar volume, which we get from Equation (19) below.

Now the partition function for a full hexagon of 6 waters is given as

$$Q_1 = (\Delta_{HB} + \Delta_{LJ} + \Delta_o)^6, \tag{14}$$

where the subscript 1 indicates a single hexagon. We treat the hexagons here in the same way as in our 2D work[39]. The total partition function for each hexagon, by taking into account also higher cooperativity in ice, is given by

$$Q_1 = (\Delta_{HB} + \Delta_{LJ} + \Delta_o)^6 - \Delta_{HB}^6 + \delta \Delta_s^6 \tag{15}$$

where $\delta = \exp(-\beta \epsilon_c)$ is the Boltzmann factor for the cooperativity energy, ϵ_c, that applies only when 6 water molecules all collect together into a full hexagonal cage. The terms on the right-side of this expression simply replace the statistical weight for each weakly hydrogen-bonded full hexagonal cage with the statistical weight for a cooperative strongly hydrogen-bonded hexagonal cage. Δ_s is the Boltzmann factor for a cooperative hexagonal cage. It differs from Δ_{HB} only in the volume per molecule, v_s instead of v_{HB}. We use Equation (15) for the whole range of temperatures; it reduces to Equation (14) in the limit of high temperatures when all cage-like structuring of water disappears.

Now we combine the Boltzmann factors for the individual water molecules to get the partition function Q for the whole system of N particles,

$$Q = Q_1^{\frac{N}{3}}, \tag{16}$$

where the factor $N/3$ accounts for all possible interaction sites per water molecule, and corrects for double-counting of the hydrogen bonds.

We compute the populations of the states $i = 1$ (HB), 2 (LJ), 3(o), 4(s) using

$$f_i = \frac{d \log Q_1}{d \log \Delta_i^6}. \tag{17}$$

The chemical potential is given by

$$\mu = -\frac{k_B T}{N} \log Q, \tag{18}$$

and the molar volume

$$v = \frac{V}{N} = \left(\frac{\partial \mu}{\partial p}\right)_T = \sum f_i v_i. \tag{19}$$

V is the total volume of the system. All the other thermodynamic properties below are obtained as described previously[48,49].

E. Solid phase

In order to compute the models solid-liquid transition we must determine the low pressure (LP) crystalline phase. Our choice is the diamond structure. This crystal structure is analogous to Ice-I crystalline phase that has been observed in low temperature Monte Carlo simulations of the 3D MB model[46,47]. We treat the model ice via a cell theory approach[48,49], assuming that the solids are incompressible. We obtained analytical expressions for the chemical potential $\mu_{LP}(T, p)$ in the same way as in hydrogen bonded state[48,49]. The molar volume v_{LP} is the same as for v_s.

III. RESULTS AND DISCUSSION

In this section, we explore the predictions of the analytical theory, for how the density, molar volume, heat capacity, isothermal compressibility and thermal expansion coefficient depend on temperature and pressure. The analytical results are compared with the Monte Carlo simulation results of 3D Mercedes–Benz water by Dias et al.[46] (and in few cases also with the experimental trends). Previous work has shown that the Mercedes–Benz water qualitatively correctly reproduces the anomalies of water[46].

For all the model calculations below, we used the following parameters: $\epsilon_{HB} = 1$, $r_{HB} = 1$, vdW: $\epsilon_{LJ} = 0.05$, $\sigma_{HB} = 0.92653$ (unchanged from Dias's 3D MB model[46]), $k_s = 78$, and

$\epsilon_c = 0.18$. We present our results below in dimensionless units, normalized to the strength of the optimal hydrogen bond ϵ_{HB} and hydrogen bond separation r_{HB} ($T^* = k_BT/\epsilon_{HB}$, $u^{ex*} = u^{ex}/\epsilon_{HB}$, $V^* = V/r_{HB}^3$, and $p^* = pr_{HB}^3/\epsilon_{HB}$).

Fig. 3 and 4 compare predictions of the present theory for the density of water and the molar volume, V^*/N, to NPT Monte Carlo simulations[46] of the 3D MB model with the same parameters. The calculations of the theory were performed at a reduced pressure of $p^* = 0.20$. The theory is in good general agreement with the simulations, including the density maximum (minima in molar volume), although the theory predicts a density maximum that is shifted (T^*=0.143) relative to the simulations ($T^* = 0.128$). This may be either due to approximations in the theory (notice that the theory is modeled roughly on the MB model) or the theory does not have exactly the same underlying Hamiltonian as simulations. Theory also predict freezing of liquid water at lower temperature (T^*=0.088) than observed in simulation (T_f^*=0.12). Data at lower temperatures present solid phase. Notice also that in Figure 3 density is plotted in same units as in Dias's work[46].

Figures 5, 6, and 7 show dependence of the thermal expansion coefficient, α^*, the isothermal compressibility, κ_T^*, and the heat capacity, C_p^*, vs. temperature. For these quantities also, the theory is in qualitative agreement with the Monte Carlo simulation results. The thermal expansion coefficient is negative at low temperatures which is consistent with computer simulations and with experiments for water. The Monte Carlo simulations of MB water do not show experimentally observed minimum in the isothermal compressibility versus temperature. On the other hand the present theory predicts minimum in κ_T^* (Fig. 6). This is consistent with scattering experiments[56]. At low temperatures, our present model shows a drop in C_p^* as the temperature is reduced.

Fig. 8a shows the model populations of the strong hydrogen-bonding state (f_s), weak hydrogen-bonding state (f_{HB}) and the state of no hydrogen bonds ($f_{LJ} + f_0$) vs temperature as obtained by this model. Fig. 8b shows corresponding experimental data for the populations of strong and weak hydrogen bonds as measured from OH stretching bands in IR spectroscopy by Luck[57]. Luck identifies three spectroscopic states: strongly-cooperative hydrogen-bonded, weakly-cooperative hydrogen-bonded, and non-bonded. We regard these three states as corresponding to the three states in our theory. Qualitatively, the trends are the same, but there is not quantitative agreement. Strong hydrogen bonds are prevalent in cold water. Heating melts the strong HB structures into structures that have a mixture of

weak hydrogen bonds, LJ interactions, and non-bonded structures at intermediate temperatures. At higher temperatures, approaching the critical point, the weak hydrogen bonds break to form non-bonded gas-phase states.

Figure 9 compares the temperature dependence of the molar volume, isothermal compressibility, κ_T^*, the thermal expansion coefficient, α^*, and the heat capacity, C_p^* from our water model to a model that is intended to describe simpler liquids: the van der Waals equation for a 3D gas. We can see that the high temperature limiting values of all calculated quantities approach the values of the van der Waals gas and when the temperature of water is above $T^* = 0.20$-0.30 the properties of water are similar to properties of van der Waals gas. Computer simulations were not done in this temperature range so we can not test this prediction with computer experiment. We can also notice small maxima in heat capacity and in compressibility in supercooled region. The dependence of the compressibility vs. T^* can be explained using Le Chateliers principle. In very cold water, the liquid is dominated by strong hydrogen bond states and its compressibility is low. As the supercooled liquid is heated, the compressibility increases because applied pressure can now force waters from strong into weak hydrogen bond states with smaller volumes. The stable liquid has a smaller compressibility than the supercooled liquid because population of states with smaller volume is higher. With increasing temperature the isothermal compressibility is high because the waters are in open states with low density.

Water expands upon freezing, $\Delta v > 0$, and the enthalpy change at freezing is negative, $\Delta h < 0$. From the Clausius-Clapeyron equation ($\frac{dp}{dT} = \frac{\Delta h}{T\Delta v}$) we get the coefficient dp/dT is negative, which means that the freezing temperature is decreasing with increasing pressure. This effect is demonstrated in Figure 10, where the model dependence of the density on temperature is shown for different values of pressure. The freezing temperature is shifting to lower values as pressure increases, confirming the result dp/dT <0. In our model we are noticing the same effect as it is seen in computer simulations by Dias et al[46].

The excess entropy per molecule, defined as the difference between the entropies of the liquid and the ideal gas under identical density and temperature conditions, was calculated as function of density at constant temperatures and results were presented in Figure 11. The excess entropy is often used as a measure of the fluids structural order. Water's excess entropy shows non-monotonic trends along isotherms at low temperature, exhibiting a density range where compression anomalously increases excess entropy[58–62]. This trend is

intimately related to water's anomalous density trends in diffusivity[58–62], shear viscosity[58,61] and thermal conductivity[58]. The interval of densities within which the excess entropy increases upon isothermal compression has been used to define a structurally anomalous region within previous studies[58–62]. For our model, at high temperatures the excess entropy of the model is monotonic function of density while at low temperatures we noticed non-monotonic trends. These trends are all at densities which correspond to liquid densities of anomalous properties.

IV. CONCLUSIONS

We developed a simple 3-dimensional model for the thermal and volumetric properties of 3D MB model of water. The model assumes three states for each water-water interaction: hydrogen bonded, or van der Waals bonded, or nonbonded, and calculations are nearly analytical. The model's properties can be computed as functions of (T, p, N) in seconds on a single CPU. It shows how Lennard-Jones attractions and repulsions are balanced against hydrogen bonding interactions differently at different temperatures and pressures. The theory predicts volumetric properties such as the temperature of maximum density, the isothermal compressibility, the thermal expansion coefficient, and water's heat capacity in good agreement with the underlying 3D Mercedes-Benz model, which was previously studied by Dias et al. by NPT Monte Carlo simulations.

ACKNOWLEDGMENTS

We appreciate the support of the Slovenian Research Agency (P1 0103–0201) and NIH Grant GM063592. Thanks to Vojko Vlachy, Barbara Hribar Lee and Miha Luksic for insightful discussions.

REFERENCES

[1]W. Röntgen, Ann. Phys. Chem. **45**, 91 (1892).

[2]J. A. Pople, Proc. Roy. Soc. A, **205**, 163 (1951).

[3]G. M. Bell, J. Phys. C: Solid State Phys., **5**, 889 (1972).

[4]A. Rahman and F. H. Stillinger, J. Chem. Phys., **57**, 4009 (1972).

[5]S. S. Borick, P. G. Debenedetti and S. Sastry, J. Phys. Chem., **99**, 3781 (1995).

[6]C. J. Roberts and P. G. Debenedetti, J. Chem. Phys., **105**, 658 (1996).

[7]C. J. Roberts, A. Z. Panagiotopoulos and P. G. Debenedetti, Phys. Rev. Lett., **77**, 4386 (1996).

[8]N. A. M. Besseling and J. M. H. M. Scheutjens, J. Phys. Chem., **98**, 11597 (1994).

[9]N. A. M. Besseling and J. Lyklema, J. Phys. Chem., **98**, 11610 (1994).

[10]C. A. Angell, J. Phys. Chem., **75**, 3698 (1971).

[11]G. Franzese, M. I. Marque and H. E. Stanley, Phys. Rev. E, **67**, 011103 (2003).

[12]G. Nemethy and H. A. Scheraga, J. Chem. Phys., **36**, 3382 (1962).

[13]A. T. Hagler, H. A. Scheraga and G. Nemethy, J. Phys. Chem., **76**, 3229 (1972).

[14]C. H. Cho, S. Singh and G. W. Robinson, Phys. Rev. Lett., **76**, 1651 (1996).

[15]T. M. Truskett, P. G. Debenedetti, S. Sastry and S. Torquato, J. Chem. Phys., **111**, 2647 (1999).

[16]G. Franzese, G. Malescio, A. Skibinsky, S. V. Buldyrev and H. E. Stanley, Nature, **409**, 692 (2001).

[17]G. Franzese, J. Mol. Liq., **136**, 267 (2007).

[18]L. Pratt and D. Chandler, J. Chem. Phys., **73**, 3430 (1980).

[19]G. Hummer, S. Garde, A. E. Garcia, M. E. Paulaitis and L. R. Pratt, J. Phys. Chem. B, **102**, 10469 (1998).

[20]G. Hummer, S. Garde, A. E. Garcia, A. Pohorille and L. R. Pratt, Proc. Natl. Acad. Sci. USA, **93**, 8951 (1996).

[21]J. A. Barker and R. O.Watts, Chem. Phys. Lett., **3**, 144 (1969).

[22]A. Rahman and F. H. Stillinger, J. Chem. Phys., **55**, 3336 (1971).

[23]F. H. Stillinger and A. Rahman, J. Chem. Phys., **60**, 1545 (1974).

[24]H. J. C. Berendsen, J. P. M. Postma, W. F. van Gunsteren and J. Hermans, *Simple point charge water*. In B. Pullman, editor, Intermolecular Forces, pages 331342, Reidel, Dordrecht (1981).

[25]W. L. Jorgensen, J. Chandrasekhar, J. D. Madura, R. W. Impey and M. L. Klein, J. Chem. Phys., **79**, 926 (1983).

[26]H. J. C. Berendsen, J. R. Grigera and T. P. Straatsma, J. Phys. Chem., **91**, 6269 (1987).

[27]M.W. Mahoney and W. L. Jorgensen, J. Chem. Phys., **112**, 8910 (2000).

[28]H. W. Horn, W. C. Swope, J. W. Pitera, J. D. Madura, T. J. Dick, G. L. Hura and T. Head- Gordon, J. Chem. Phys., **120**, 9665 (2004).

[29]J. Caldwell, L. X. Dang and P. A. Kollman, J. Am. Chem. Soc., **112**, 9144 (1990).

[30]S.W. Rick, S. J. Stuart and B. J. Berne, J. Phys. Chem., **101**, 6141 (1994).

[31]H. Yu, T. Hansson and W. F. van Gunsteren, J. Chem. Phys., **118**, 221 (2003).

[32]P. Ren and J.W. Ponder, J. Phys. Chem. B, **107**, 5933 (2003).

[33]I.-F. W. Kuo and C. J. Mundy, Science, **303**, 658 (2004).

[34]A. G. Donchev, N. G. Galkin, A. A. Illarionov, O. V. Khoruzhii, M. A. Olevanov, M. V. Subbotin and V. I. Tarasov, Proc. Natl. Acad. Sci. USA, **103**, 8613 (2006).

[35]R. Bukowski, K. Szalewicz, G. C. Groenenboom and A. van der Avoird, Science, **315**, 1249 (2007).

[36]L. A. Baez and P. Clancy, J. Chem. Phys., **103**, 9744 (1995).

[37]M. Yamada, S. Mossa, H. E. Stanley and F. Sciortino, Phys. Rev. Lett., **88**, 195701(2002).

[38]C. J. Fennell and J. D. Gezelter, J. Chem. Theory Comput., **1**, 662 (2005).

[39]T. Urbic and K. A. Dill, J. Chem. Phys. **132**, 224507 (2010).

[40]A. Ben-Naim, J. Chem. Phys. **54**, 3682 (1971).

[41]A. Ben-Naim, Mol. Phys. **24**, 705 (1972).

[42]A. Ben-Naim, *Water and Aqueous Solutions* (Plenum Press, New York, 1974).

[43]A. Ben-Naim, *Molecular Theory of Water and Aqueous Solutions, 1st ed.* (World Scientific, Singapore, 2009).

[44]A. Bizjak, T. Urbic, V. Vlachy, and K. A. Dill, Acta Chim. Slov. **54**, 532 (2007).

[45]A. Bizjak, T. Urbic, V. Vlachy and K. A.Dill, J. Chem. Phys. **131**, 194504 (2009).

[46]C. L. Dias, T. Ala-Nissila, M. Grant and M. Karttunen, J. Chem. Phys. **131**, 054505 (2009).

[47]C. L. Dias, T. Hynninen, T. Ala-Nissila, A. S. Foster and M. Karttunen, J. Chem. Phys. **134**, 065106 (2011).

[48]T. M. Truskett and K. A. Dill, J. Chem. Phys., **117**, 5101 (2002).

[49]T. M. Truskett and K. A. Dill, J. Phys. Chem. B, **106**, 11829 (2002).

[50]K. A. Dill, T. M. Truskett, V. Vlachy and B. Hribar-Lee, Annu. Rev. Biophys. Biomol. Struct., **34**, 173 (2005).

[51]P. H. Poole, F. Sciortino, T. Grande, H. E. Stanley and C. A. Angell, Phys. Rev. Lett., **73**, 1632 (1994).

[52]C. J. Roberts and P. G Debenedetti, J. Chem. Phys., **105**, 658 (1996).

[53]M. Pretti, C. Buzano and E. De Stefanis, J. Chem. Phys., **131**, 224508 (2009).

[54]M. Lukšič, T. Urbic, B. Hrebar-Lee and K. A. Dill, J. Phys. Chem. B, **116** 6177 (2012).

[55]E. A. Jagla, J. Chem. Phys. **111**, 8980 (1999).

[56]C. Huang, K. T. Wikfeldt, T. Tokushimc, D. Nordlund, Y. Harada, U. Bergmann, M. Niebuhr, T. M. Weiss, Y. Horikawa, M. Leetmaa, M. P. Ljungberg, O. Takahashi, A. Lenz, L. Ojamae, A. P. Lyubartsev, S. Shin, L. G. M. Pettersson, and A. Nilsson, Proc. Natl. Acad. Sci. USA , (2009).

[57]W. A. P. Luck, J. Mol. Struct. **448**, 131 (1998).

[58]J. R. Errington, T. M. Truskett, and J. Mittal, J. Chem. Phys., **125**, 244502 (2006).

[59]J. Mittal, J. R. Errington, and T. M. Truskett, J. Chem. Phys., **125**, 076102 (2006).

[60]R. Sharma, S. N. Chakraborty and C. Chakravartya, J. Chem. Phys., **125**, 204501 (2006).

[61]R. Chopra, T. M. Truskett, and J. R. Errington, J. Phys. Chem. B, **114**, 10558 (2010).

[62]M. Agarwal, M. Singh, R. Sharma, M. P. Alam and C. Chakravarty, J. Phys. Chem. B, **114**, 6995 (2010).

CAPTIONS TO THE FIGURES.

Figure 1. The lattice of the model showing both the hexagon of the ice-like structure and showing illustrating a pair interaction used for bookkeeping to avoid triple-counting. Presented is only one layer.

Figure 2. The three model states: (1) hydrogen-bonded, (2) van der Waals, and (3) non-bonded.

Figure 3. (Color online) Temperature dependence of the density at $p^* = 0.20$: Theory (line) *vs.* Monte Carlo simulation of the MB model[46] (symbols). Notice also that density is plotted in same units as in Dias's work[46].

Figure 4. (Color online) Temperature dependence of the molar volume coefficient; legend otherwise as for Fig. 3.

Figure 5. (Color online) Temperature dependence of the thermal expansion coefficient; legend otherwise as for Fig. 3.

Figure 6. (Color online) Temperature dependence of the isothermal compressibility; legend otherwise as for Fig. 3.

Figure 7. (Color online) Temperature dependence of the heat capacity at constant pressure; legend otherwise as for Fig. 3.

Figure 8. (Color online) (a) Temperature dependence of the populations, f_i of the different type of hydrogen bonds, at constant pressure, $p^* = 0.19$. The population of strong hydrogen bonds (long dashed line), weak hydrogen bonds (solid line), no hydrogen bonds (short dashed line). (b) Experimental populations of OH states in liquid water vs. temperature T_r[48] along its saturation curve, from IR spectroscopic data (adapted from Fig. 5 of Luck[57]).

Figure 9. (Color online) Temperature dependence of the molar volume (a), heat capacity (b), isothermal compressibility (c) and thermal expansion coefficient (d) at $p^* = 0.2$: theory (solid line), and van der Waals 3D gas (dashed line).

Figure 10. (Color online) Temperature dependence of the reduced density at different values of pressure, $p^* = 0.2$ solid line, $p^* = 0.16$ long dashed, $p^* = 0.12$ dashed and $p^* = 0.08$ dash-dotted line.

Figure 11. (Color online) Density dependence of the excess entropy at different temperatures, $T^* = 0.25$ solid line, $T^* = 0.20$ long dashed, $T^* = 0.15$ dashed and $T^* = 0.12$ dash-dotted line.

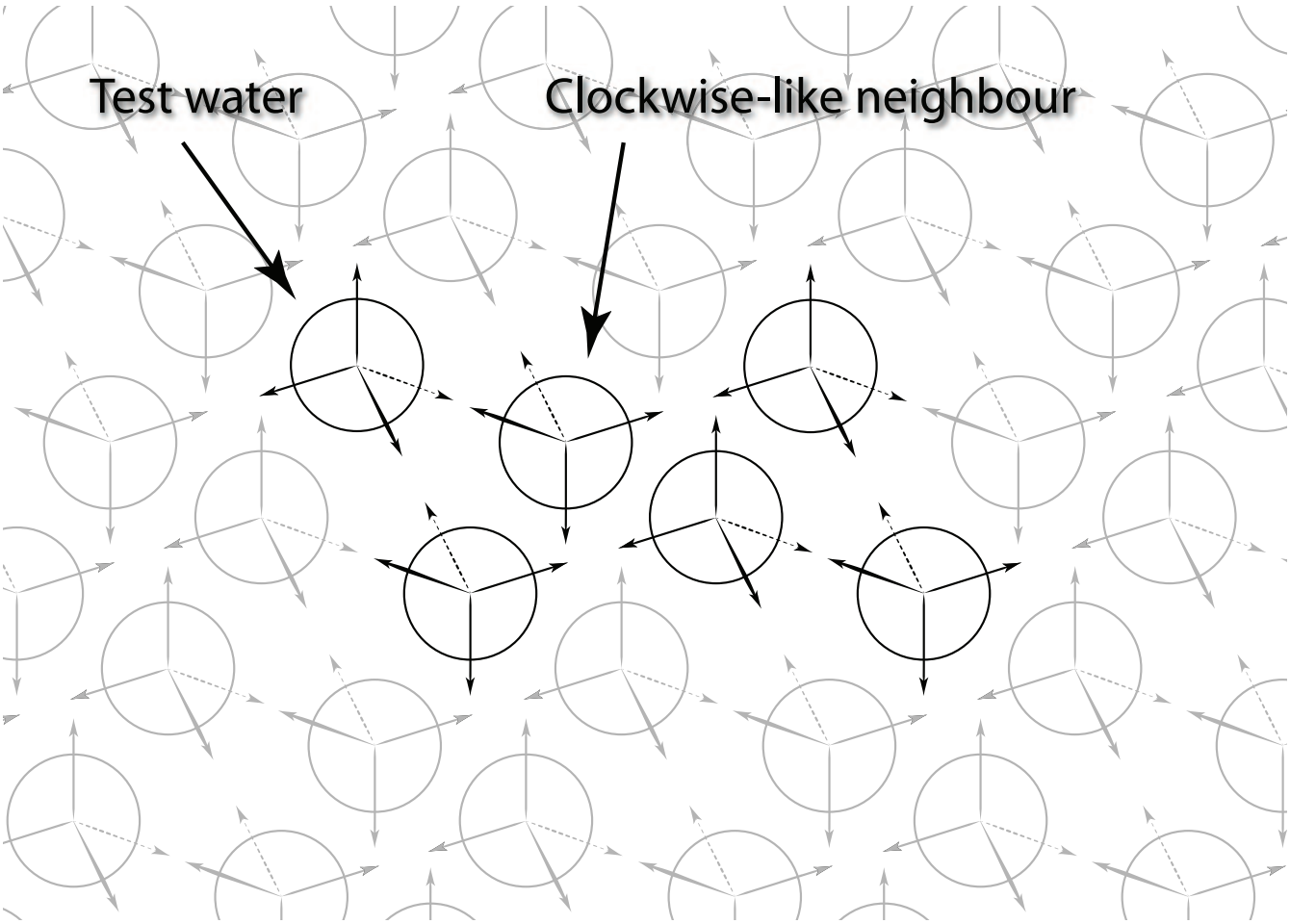

Figure 1 ES10798 13Jun2012

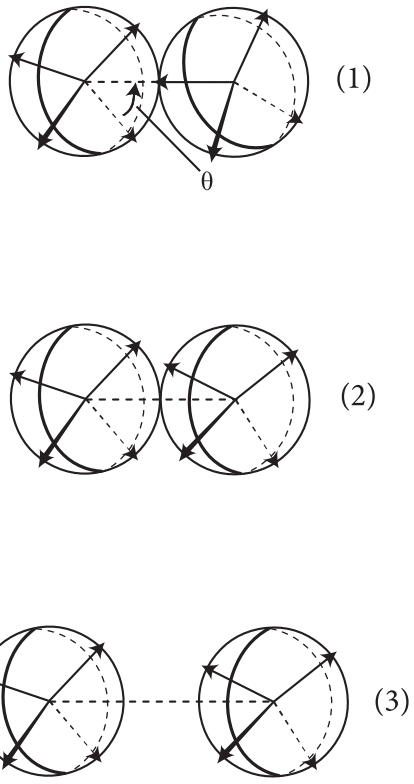

Figure 2 ES10798 13Jun2012

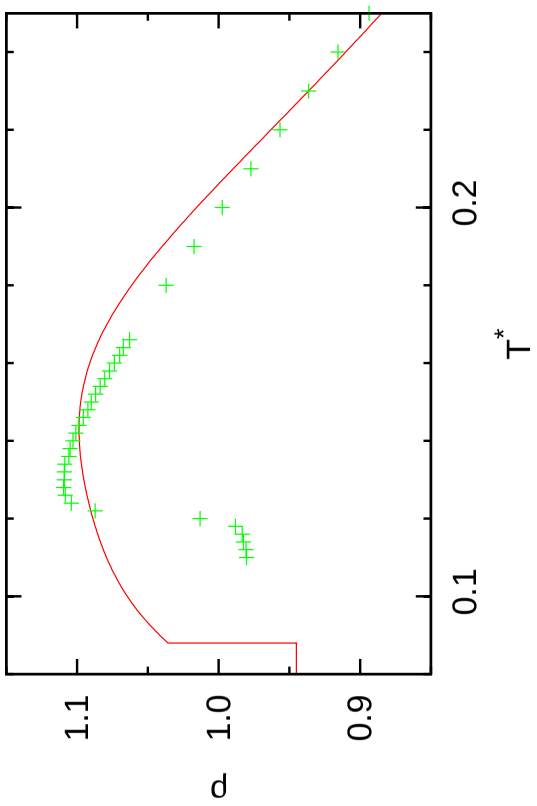

Figure 3 ES10798 13Jun2012

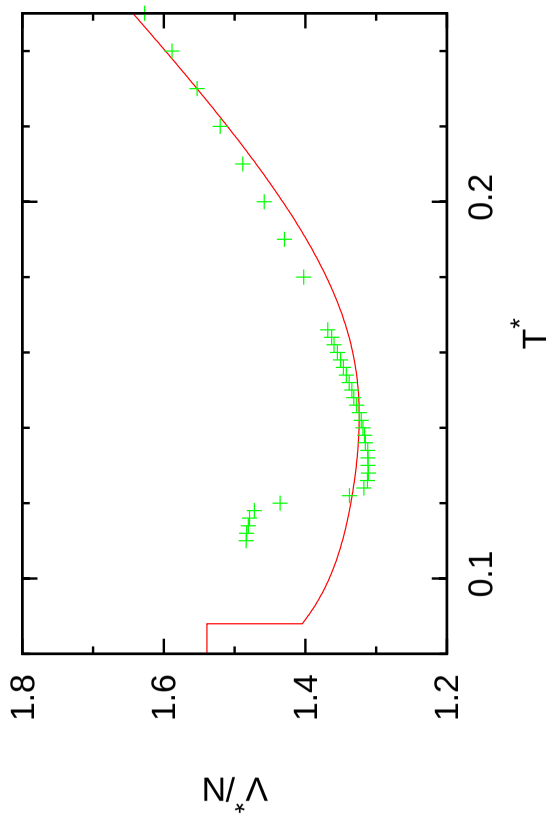

Figure 4 ES10798 13Jun2012

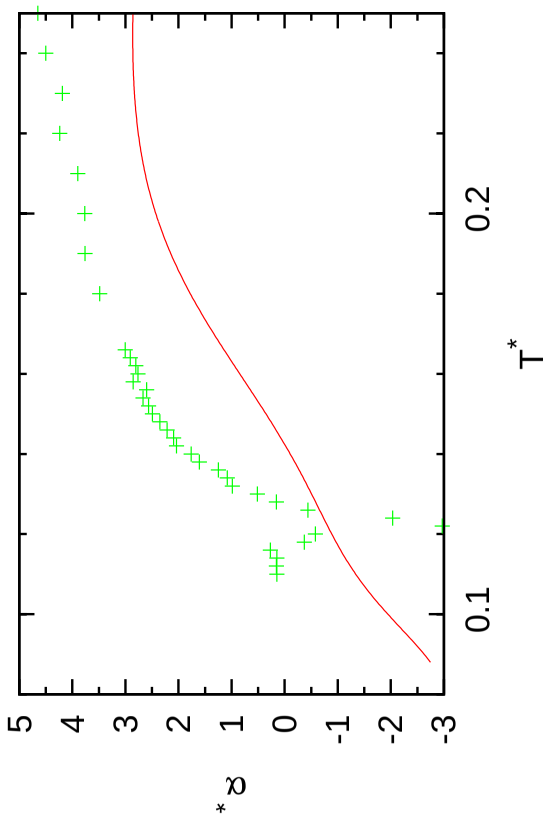

Figure 5 ES10798 13Jun2012

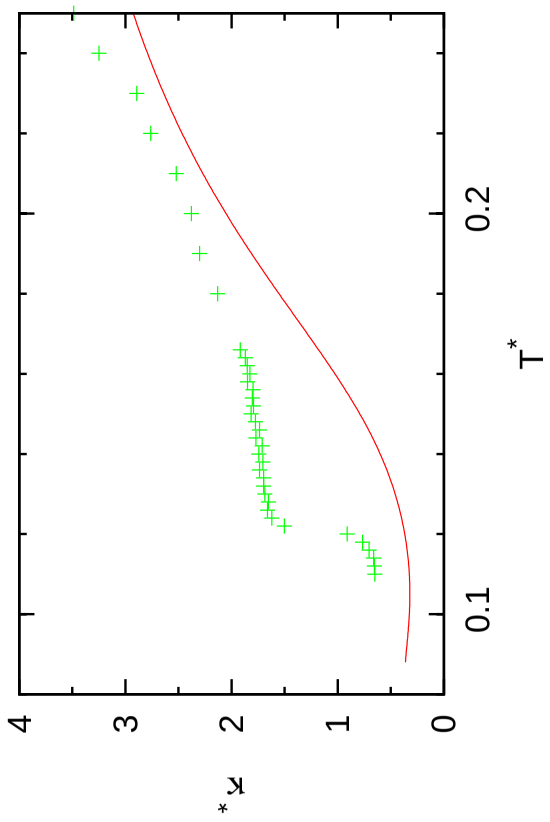

Figure 6 ES10798 13Jun2012

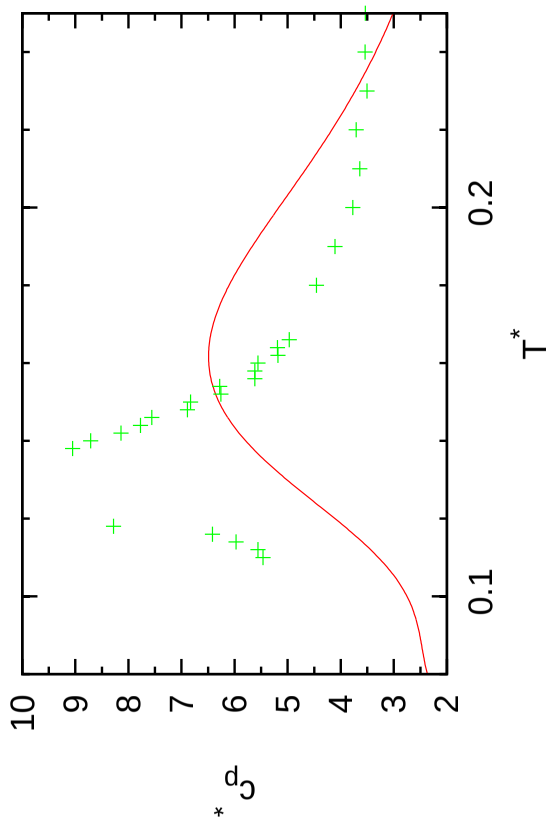

Figure 7 ES10798 13Jun2012

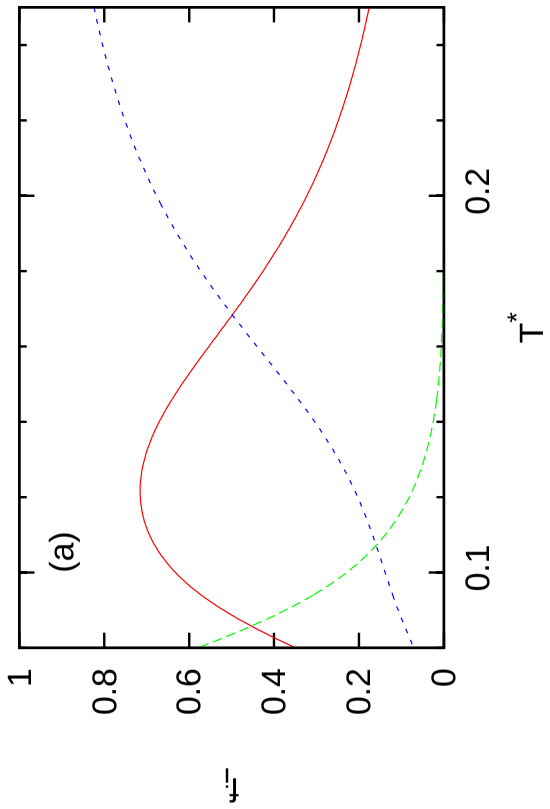

Figure 8a ES10798 13Jun2012

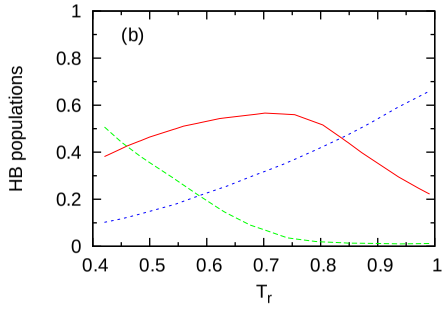

Figure 8b ES10798 13Jun2012

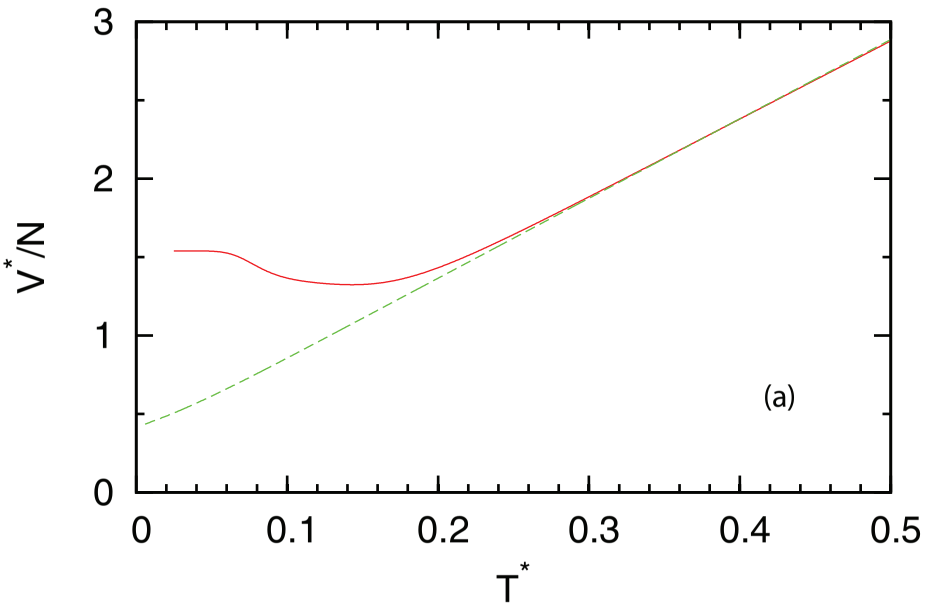

Figure 9a ES10798 13Jun2012

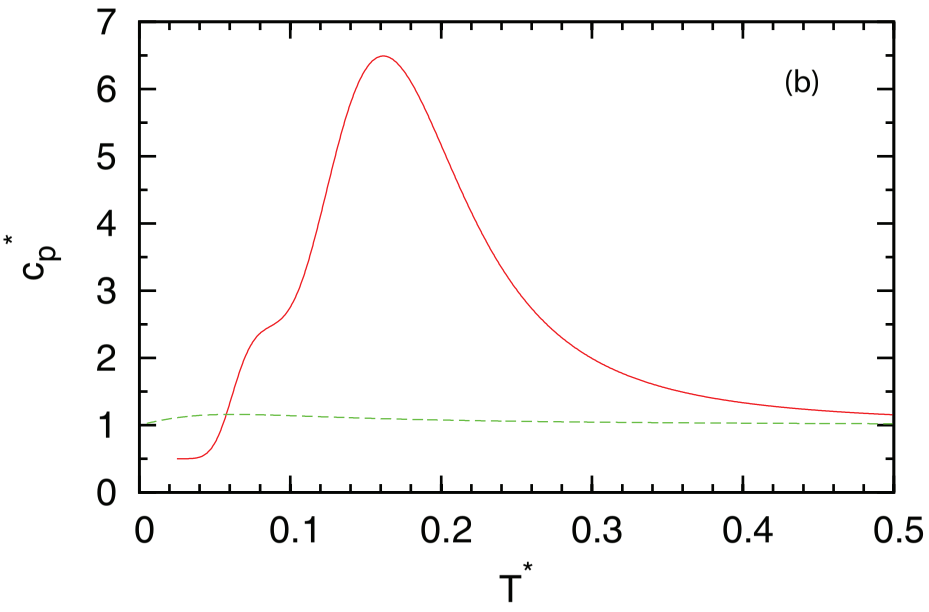

Figure 9b ES10798 13Jun2012

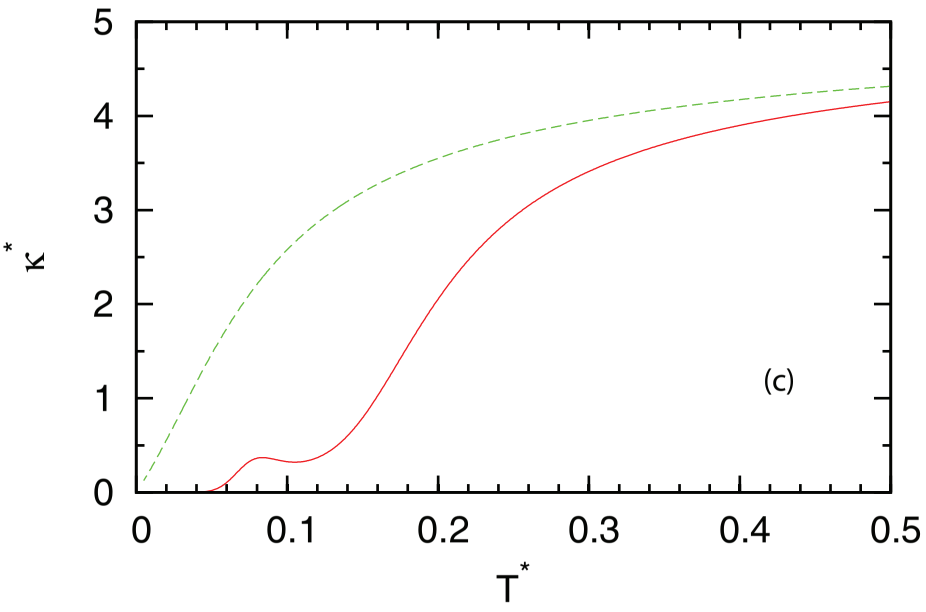

Figure 9c ES10798 13Jun2012

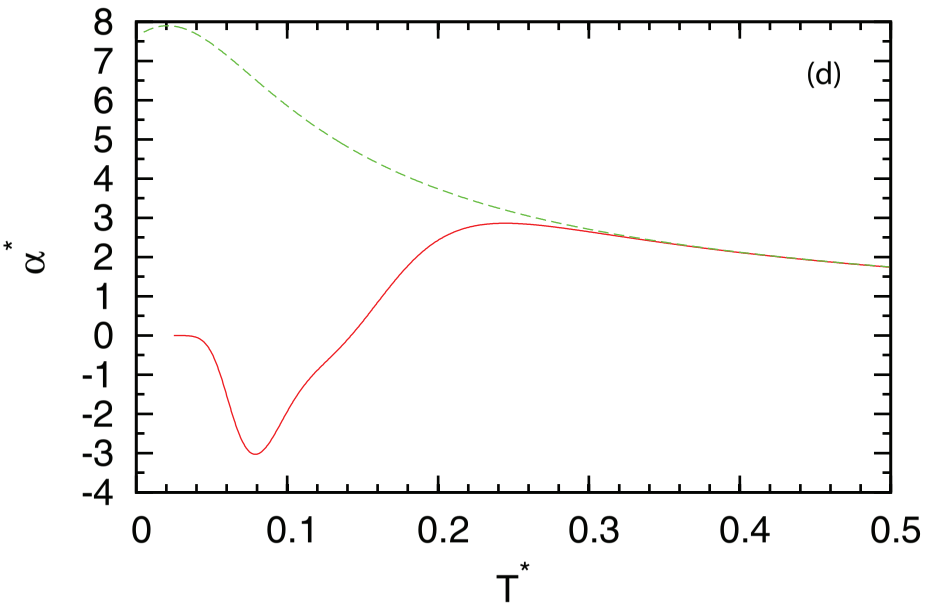

Figure 9d ES10798 13Jun2012

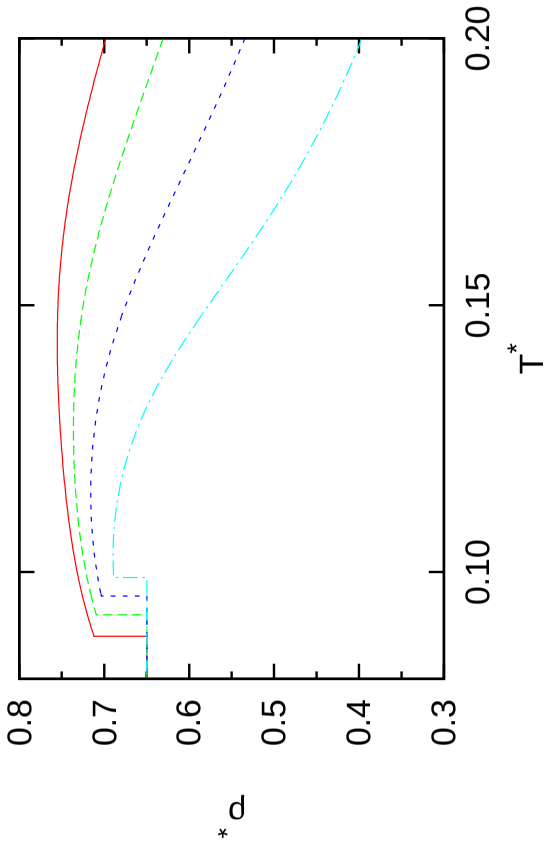

Figure 10 ES10798 13Jun2012

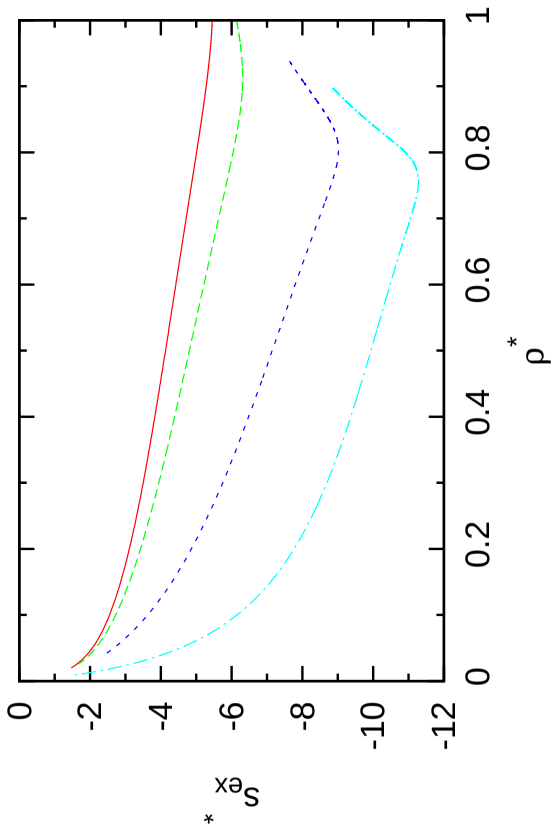

Figure 11 ES10798 13Jun2012